ISSN 0016-7029, Geochemistry International, 2010, Vol. 48, No. 7, pp. 643–654. © Pleiades Publishing, Ltd., 2010.
Original Russian Text © A.A. Novoselov, S.A. Silantyev, 2010, published in Geokhimiya, 2010, Vol. 48, No. 7, pp. 685–697.

Hydrothermal Systems of the Hadean Ocean and Their Influence on the Material Balance in the Crust–Hydrosphere–Atmosphere System of the Early Earth

A. A. Novoselov and S. A. Silantyev

Vernadsky Institute of Geochemistry and Analytical Chemistry, Russian Academy of Sciences, ul. Kosygina 19, Moscow, 119991 Russia;
e-mail: elevfaniy@rambler.ru

Received December 9, 2008

Abstract—This paper reports the first results of kinetic and thermodynamic modeling of interaction between the komatiitic material of the earliest terrestrial ocean and seawater. The modeling was aimed at reconstructing geochemical effects accompanying the early evolution of the earth's outer shells, atmosphere, and hydrosphere. We also explored the character of mineral transformations in the protooceanic crust during its hydrothermal alteration. Kinetic and thermodynamic simulation by means of the GEOCHEQ program complex was the main tool of our study. The results of modeling allowed us to estimate the character of the environment and the duration of the formation of the oldest banded iron formation (BIF) and volcanogenic massive sulfide (VMS) deposits and reconstruct main trends in the compositional variations in the hydrosphere and atmosphere that coexisted with them.

DOI: 10.1134/S0016702910070025

INTRODUCTION

The basic idea for this study evolved from the suggestion that the lithology of the earth's primitive protocrust and the character of processes occurring during its formation were similar to those in present-day ocean basins. The modern oceanic crust is the most primitive of the existing geochemical types of crustal reservoirs. Only in modern ocean basins, magmatic, metamorphic, and hydrothermal processes are very closely spaced in time and, similar to the oldest Hadean ocean, probably controlled by contributions from the minimum number of main planetary reservoirs, including the suboceanic mantle, oceanic crust, and oceanic hydrosphere. Therefore, the processes occurring during the accretion of the modern oceanic crust are formally similar to those responsible for the formation of the earth's protocrust and are probably different from them only in physicochemical parameters.

The protocrust–hydrosphere system was formed on earth already during the earliest 50–150 Ma of its existence [1, 2], immediately after the separation of the major volume of its core from the primordial material of the earth [3]. It can be supposed that the crustal material of the Hadean ocean underwent hydrothermal alteration during the several hundreds of million years of the existence of this system (approximately 700–800 Ma according to [4]). Mineralogical and isotope geochemical data indicating the possible participation of hydrothermal fluid of marine origin in the formation of the earliest oceanic crust in the Archean were discussed in [5–9]. Some authors argued that all Archean massive sulfide occurrences were formed owing to the activity of marine hydrothermal systems (e.g., [8]). Thus, there are grounds to assume that the Hadean ocean comprised active hydrothermal fields, which are also an ubiquitous geological indicator of the modern global system of mid-ocean ridges (MOR).

One promising approach to reconstructing the geochemical and physicochemical characteristics of oceanic hydrothermal systems is physicochemical modeling. Based on the data on the possible composition of the Hadean oceanic protocrust under variable T, P, t, and W/R (water/rock weight ratio) parameters controlling the phase composition of rocks and the composition of fluid interacting with them, this method can be used to assess geochemical effects related to the activity of the oldest hydrothermal systems on earth. This approach was used in this study.

MODELING TECHNIQUE

Kinetic and thermodynamic simulation by means of the GEOCHEQ program complex [10] was the main tool of our study. Irreversible chemical interactions between ultrabasic rocks and aqueous solutions were investigated using a model involving the description of the kinetics of mineral dissolution and the calculation of the equilibrium composition of the system at each time step. The occurrence of chemical reactions was modeled as a series of sequential equilibrium states at each time step. The current chemical balance of the system was computed from the chemical balance of aqueous solution at the previous

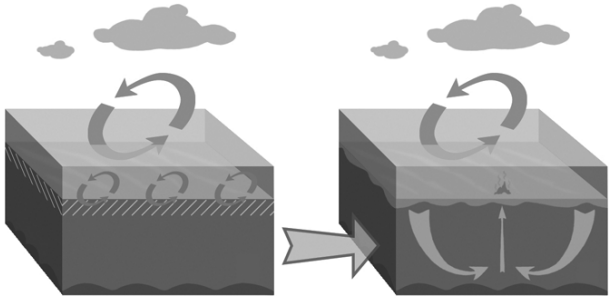

Fig. 1. Stages of modeling reproducing possible scenarios for the evolution of the chemical composition of the outer geospheres: (1) low-temperature alteration of crystalline rocks owing to their interaction with seawater and (2) medium- to high-temperature alteration of crystalline rocks owing to their interaction with hydrothermal fluid.

step and the current rates of mineral dissolution. The molar amount of a mineral dissolved at each step was specified as $x_i = Fs_i S_i r_i \Delta t$, where S_i is the current surface area of the ith mineral; $r_i = f_i(\text{pH}, T, G_i)$ is the current rate of mineral dissolution, mol cm^{-2} sΔt ; and Δt is the time step size, s. The multiplier Fs_i $(0 < Fs_i < 1)$ accounts for the degree of accessibility of the mineral surface to the aqueous solution. The minerals that precipitated during previous steps were considered as primary and could subsequently be dissolved if they appeared out of equilibrium with the current composition of aqueous solution. The model and its prospects and limitations were described in detail in [11].

Modeling included two stages (Fig. 1) corresponding to two possible scenarios of the evolution of the chemical composition of the outer geospheres: (1) low-temperature alteration of crystalline rocks under the influence of seawater and (2) medium- to high-temperature transformation of crystalline rocks owing to their interaction with hydrothermal fluid. In the latter case, the modeling of the downwelling limb of the Hadean hydrothermal system was carried out for two variants of rock–fluid interaction corresponding to different W/R (water/rock) ratios on the surface: 1 and 10. In this study, we used the same concept of the hydrodynamics of a model system that was described in [12].

Table 1. Composition of volcanic gases from Surtsey Volcano, Iceland, mol %

H_2O	87.88
H_2	3.12
CO_2	6.43
CO	0.39
SO_2	2.72
S_2	0.1
H_2S	0.63
HCl	0.43

RESULTS OF MODELING

The investigation of aqueous solution–rock interaction at the early stage of earth evolution is hindered by the absence of reliable estimates for the chemical compositions of waters in the hydrosphere. However, it can be supposed that the chemistry of outer geospheres was controlled during that period mainly by the mantle reservoir. Therefore, in this study, we considered the modern volcanic gas as a source for the atmosphere and hydrosphere analogous to the corresponding reservoirs of the early earth. The composition of gases from Surtsey Volcano, Iceland, [13] was used for our modeling (Table 1). This choice was motivated by the geodynamic setting of Iceland in the axis of a mid-ocean ridge. A radiative equilibrium temperature of 15°C [14] was used as the earth's surface temperature. Pressure was taken to be 1 bar. The calculation of the equilibrium composition of volcanic gases from Surtsey Volcano under given P–T conditions yielded the compositions of aqueous solution (Table 2) and gas phase consisting of CO_2 and minor amounts of water vapor.

Such an acidic and cation-free hydrosphere could not exist for any significant time period on the earth's surface and had to react with the crystalline rocks of the basement of the earliest basins during low-temperature submarine weathering. In turn, these processes had to modify the compositions of the atmosphere and hydrosphere.

Submarine Weathering on the Hadean Ocean Floor

In order to reconstruct the submarine weathering of rocks on the floor of the oldest water basins, kinetic thermodynamic modeling was performed. The composition of peridotite komatiite sample M620 (Munro Township, Archean Abitibi greenstone belt, Canada) reported in [15] was used in the calculations (wt %): 46.28 SiO_2, 7.60 Al_2O_3, 11.90 FeO*, 27.67 MgO, 6.44 CaO, and 0.11 Na_2O. The *Fs* parameter used in the calculations to account for the degree of accessibility of mineral surface to aqueous solution (see above) can be interpreted in terms of rock disintegration, microfracturing, effective porosity, etc. The real compositions of rock-forming olivine, orthopyroxene, clinopyroxene, and spinel were accepted for calculations. The sizes of mineral grains were taken to be 0.1 mm for spinel, 1.0 mm for other primary minerals, and 0.005 mm for secondary minerals. The value of *Fs* was set at 0.0005.

The initial compositions of aqueous solution and atmosphere were approximated by the compositions obtained at the previous computation stage. The W/R value was 10 and 1. The duration of interaction in the

water–rock system was 100 million model years. The temperature at the ocean floor was taken to be 15°C.

Calculations at the given temperature and W/R = 10 showed that an SiO_2-rich chemogenic envelope is already formed during the initial stage (1000 model years) of komatiite–seawater interactions on the surface of the crust of the ancient ocean basin. This alteration product is strongly dominated by amorphous silica and contains pyrite and, after 10 000 model years, goethite and Fe-chlorite (Fig. 2a). Magnetite and dolomite appear after 100 000 model years in the altered komatiite material and are followed by magnesite. Such a secondary mineral association corresponds to the phase composition of the banded iron formation (BIF) of the Early Archean. The primary minerals of the surface layer of the komatiitic crust are dissolved most intensely within 1000 model years starting from the onset of its interaction with seawater. Spinel and clinopyroxene (the most persistent primary phases of this material) are almost completely dissolved within approximately 10 million model years.

In the aqueous solution, the contents of dissolved H_2S and NH_3 decrease and that of CH_4 increases 4000 model years after the beginning of interaction (Fig. 2b). Simultaneously, the pH value of the hydrosphere increases significantly from 0.44 to 5.5. The calculations showed that after only the first 100 model years of aqueous solution–komatiite interaction result in the appearance of significant concentrations of cations in the solution composition (Fig. 2c). After 1000 model years of interaction, the maximum concentrations were obtained for Mg, Fe, and Ca. The extensive migration of Na from the protocrust to the hydrosphere occurs 100 000 model years after the beginning of submarine weathering.

According to the results of our calculations, the composition of the primordial atmosphere in equilibrium with the hydrosphere produced by gas condensation changes dramatically after 5000 model years. The atmosphere is significantly depleted in H_2S and SO_2 and slightly enriched in H_2, CH_4, and NH_3 at that time.

The modeling of submarine weathering at W/R = 1 showed that the formation of a SiO_2-rich material under such conditions requires a longer period of water–komatiite interaction (100 000 model years) compared with the model system with W/R = 10. At low W/R values, the protocrust–hydrosphere interaction produces pyrite after only 100 model years, goethite and Fe-chlorite after 150–200 model years, and magnetite and dolomite after 10 000 model years (Fig. 3a). Mg-saponite and clinochlore are formed in the rocks 100 000 model years after the beginning of interaction. This time corresponds also to the most intense deposition of carbonates.

A fundamental difference of the mineralogy of the model system with low W/R values from high-W/R systems is the appearance of serpentine (chrysotile) after 1 million of model years and talc after 10 million model years; these minerals are not formed in the model system with W/R = 10 even after 100 million model years (Fig. 3a).

Table 2. Calculated composition of the primordial hydrosphere, mol/kg H_2O

$CO_2 + HCO_3^- + CO_3^{2-}$	2.88E-02
CH_4	9.54E-25
CO	1.03E-18
$H_2S + HS^-$	5.76E-07
$HSO_4^- + SO_4^{2-}$	2.68E-01
$NH_3 + NH_4^+$	1.51E-03
H_2	3.57E-15
HCl	1.37E-02
Cl^-	2.47E-01
pH	0.44

At W/R = 1, the abundances of dissolved gases in the hydrosphere change faster compared with the high-W/R system: the contents of dissolved H_2S and NH_3 decrease and that of CH_4 increases already after 150–200 model years. Within the same time interval (at low W/R), the pH of the hydrosphere changes from 0.44 to 5.5. Similar to the higher W/R system, a significant increase in the concentrations of cations (Mg, Fe, Ca, and Na) is observed in the system with W/R = 1 in a few hundreds of years of interaction between primary seawater and the komatiitic crust. However, in contrast to relatively deep water conditions (W/R = 10), the concentration of solution in a shallow basin increases much faster, and a higher Na content is reached. According to the results of calculations for 5 Ma of interaction, the Na content in the water of a shallow basin (W/R = 1) is an order of magnitude higher than that obtained for the model system with W/R = 10. Starting from 1 million model years, the content of Mg in seawater decreases, which corresponds to the onset of komatiite serpentinization.

The composition of the atmosphere in equilibrium with the hydrosphere in the system with W/R = 1 changes significantly within only a few hundred of model years of interaction. During this period, the contents of H_2S and SO_2 in the atmosphere decrease and those of H_2, CH_4, NH_3, and CO increase slightly. After 100 000 model years of low-temperature interaction in the komatiite–hydrosphere system, a dramatic decrease in CO_2 content begins in the primordial atmosphere. It should be emphasized that this time corresponds to the beginning of extensive carbonate precipitation in the model system (Fig. 3b).

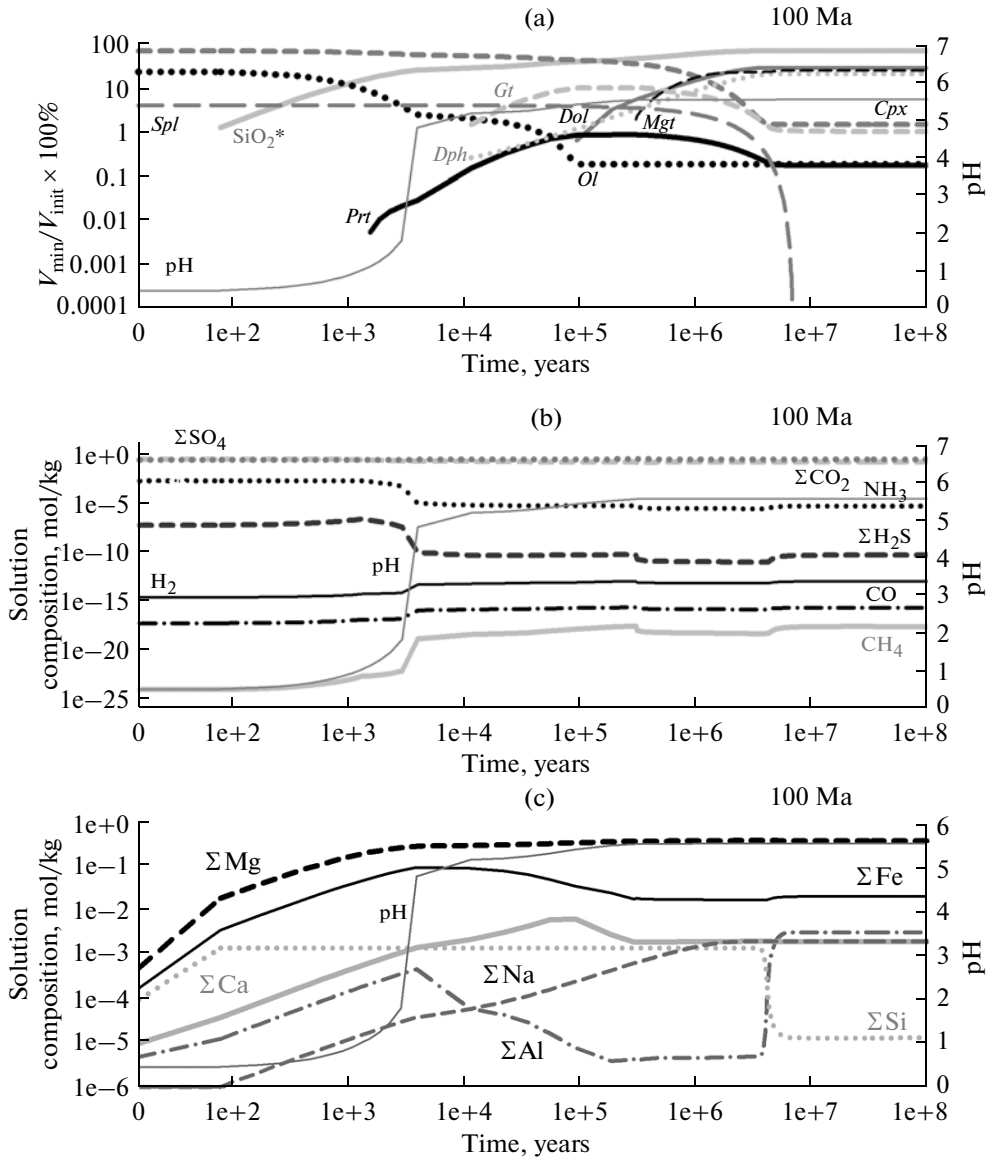

Fig. 2. (a) Phase transformations in a komatiitic material at its low-temperature interaction with the primordial hydrosphere in the model system with W/R = 10 (mineral symbols are given in the notes to Table 3). (b) Variations in the content of dissolved gases. (c) Variations in the contents of cations in the primordial hydrosphere at its low-temperature interaction with a komatiitic material.

Geochemical Effects of Hydrothermal Circulation within the Hadean Protocrust

The characteristics of mineral transformations in the Hadean protooceanic crust and the compositional evolution of hydrothermal fluid during its percolation through the komatiitic crust were investigated within a wide range of *P*–*T*–t conditions. The chemistry of the crust corresponded to the composition of unaltered peridotite komatiite presented above. The compositions of seawater used in the calculations were obtained at the previous stage of modeling. The sequential passage of five waves of hydrothermal fluid through the crustal section was considered under the following assumption: (1) the hydrothermal system has the shape of an inverted cone whose apex lies at a depth of approximately 6100 m within the crustal section, (2) the catchment area on the surface of the ancient ocean is 100 km^2, (3) the seawater flow percolates downward through the komatiite sequence focusing at the axis of the hydrothermal cell in its root part and discharges on the surface as an upwelling flow from a depth of 6100 m, and (4) pressure is equal to the hydrostatic pressure of the water body on the bottom surface and increases downward with increasing lithostatic load (ρ = 3.2 g/cm^3).

It was found that the most significant geochemical and mineralogical effects in the model system coincided with the passage of the second wave. Therefore, the modeling results discussed below refer to the second wave of hydro-

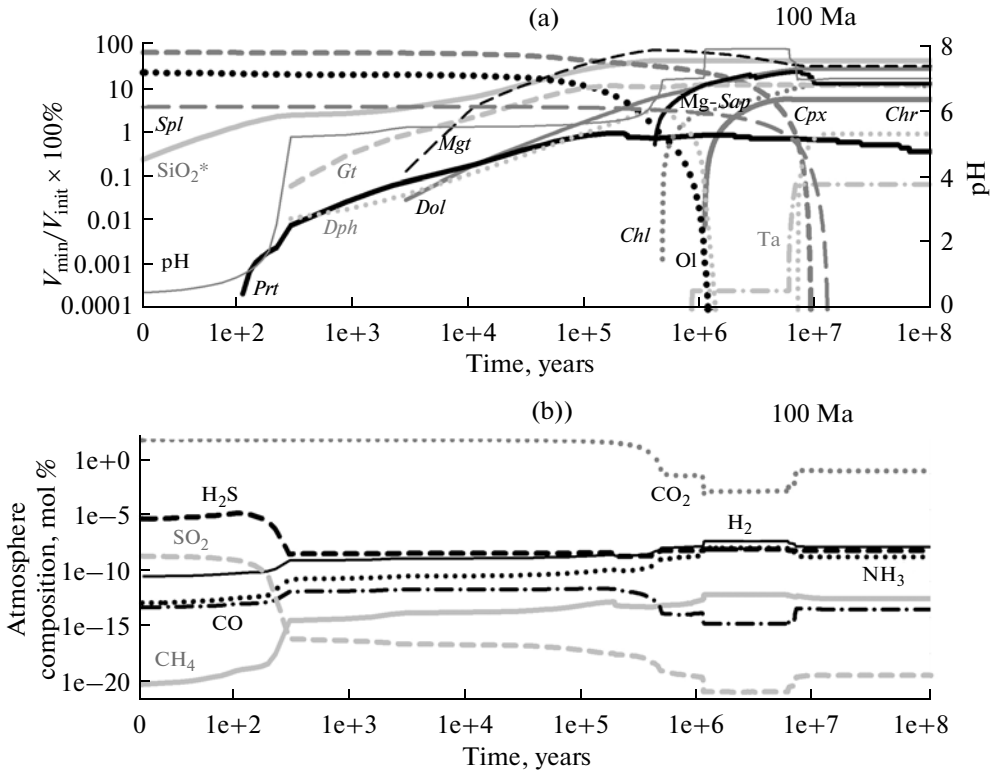

Fig. 3. (a) Phase transformations in a komatiitic material at its low-temperature interaction with the primordial hydrosphere in the model system with W/R = 1 (mineral abbreviations are given in the notes to Table 3). (b) Variations in the composition of the primordial atmosphere in equilibrium with the hydrosphere interacting with a komatiitic material at W/R = 1.

thermal fluid. Two variants of the model system with surface W/R ratios of 10 and 1 were considered.

W/R = 10, downwelling limb

Table 3 shows calculated mineral transformations for the infiltration of the second wave of hydrothermal fluid through a 6-km-thick komatiitic section. In the upper part of the section to a depth of approximately 1000 m, amorphous silica precipitates intensely and associates with goethite, pyrite, Fe- chlorite (daphnite), and magnesite at a depth of 500 m. At deeper levels (≥1000 m), quartz coexists with hematite and Mg-saponite. Serpentine (chrysotile) appears in the section at a depth of approximately 1500 m and a temperature of 116°C.[1] At the same level, hematite is replaced by magnetite. Deeper (approximately 2000 m and T = 156°C), Ca-amphibole (actinolite–tremolite) and brucite are formed in the hydrated komatiite section; these minerals are further traced up to the root (highest temperature) parts of the downwelling limb of the model hydrothermal system. Pyrrhotite appears at a depth of 2500 m (197°C). When the depth of the section reaches 3500 m, which corresponds to a model temperature of 278°C, chrysotile is replaced by antigorite, which associates with magnetite to depths of approximately 5100 m and a temperature of ~ 400°C. Starting from a temperature of 318°C (~4100 m), fayalite (iron-rich olivine) appears in the hydrothermally altered komatiite, and talc joins it at a deeper level of 4600 m (360°C). The magnetite + fayalite + talc association persists up to the root part of the downwelling limb of the hydrothermal system (439°C and 5600 m).

The results of modeling provide insight into the compositional evolution of hydrothermal fluid within the whole P–T range considered above (Fig. 4). Low-temperature interaction with komatiite in the upper part of the section (500–1000 m and 35°–75°C) is accompanied by an increase in the contents of dissolved H_2S, CH_4, and H_2 and a decrease in SO_4 in the hydrothermal fluid. The intense formation of reduced dissolved gases begins at 1500–2000 m (116–156°C). This depth level corresponds to a change of hematite by magnetite and chrysotile appearance in the rock. In the upper part of the section, the carbonate ions of hydrothermal fluid are consumed for magnesite and calcite formation. Starting from 76°C, the concentrations of Mg, Fe, and Ca in the fluid decrease, whereas that of Na increases monotonously. The dramatic removal of Mg from the fluid is observed in the section at temperatures of 116°–197°C (1500–2500 m), when solu-

[1] Hereafter, the presented temperature and pressure values are averages for model blocks and do not define the boundaries of mineral associations.)@

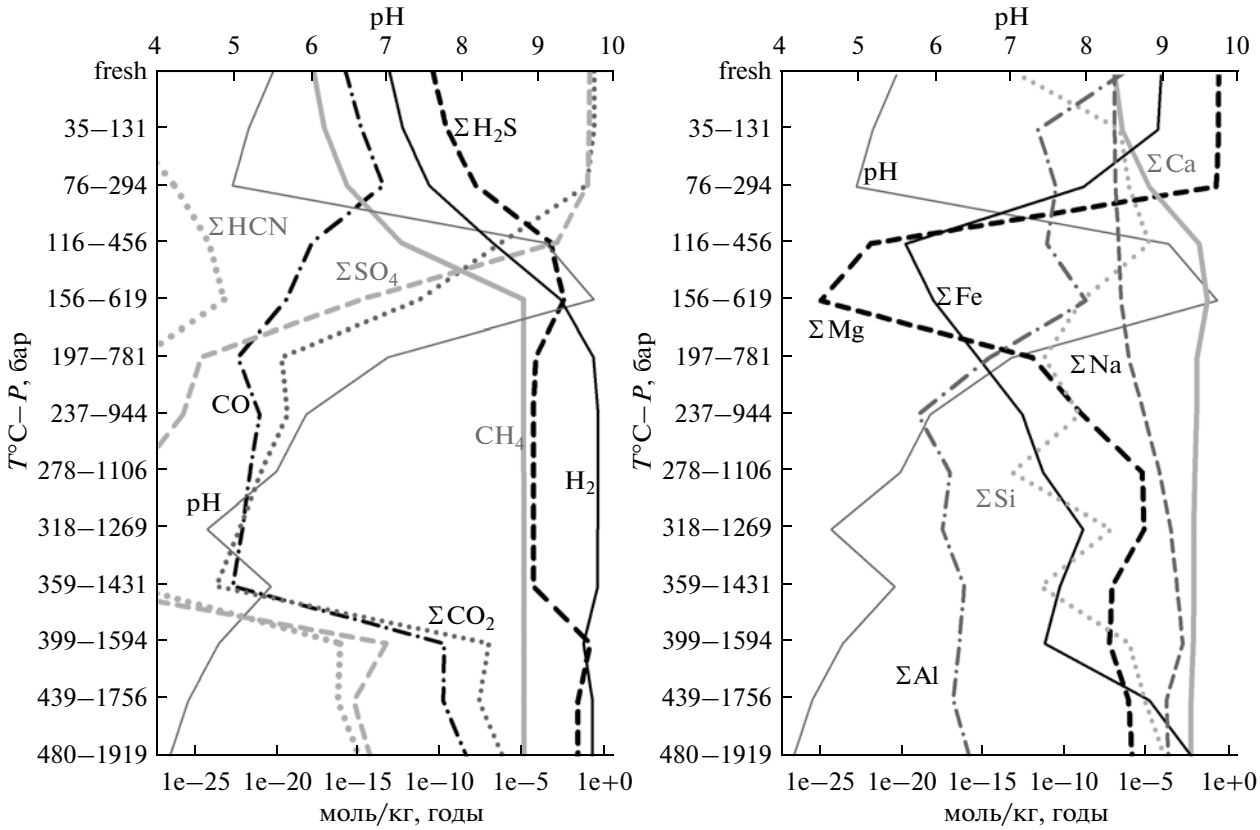

Fig. 4. Evolution of the composition of hydrothermal fluid at the downwelling limb of a hydrothermal system interacting with a komatiitic section (model system with W/R = 10 on the surface).

tion pH increases notably. The extensive serpentinization of komatiite begins at the same depths. In the highest temperature root part of the downwelling limb of the model system, the concentrations of Mg, Fe, and Na increase again.

W/R = 1, downwelling limb

In contrast to the model system with W/R = 10, the hydrothermal alteration of komatiitic material at a lower W/R value produces, in addition to goethite and pyrite, magnesium aluminosilicates clinochlore and Mg-saponite in the upper part of the section at the absence of amorphous silica (Table 4). At a depth of approximately 1000 m and a temperature of 76°C, dolomite is the only carbonate to appear, and goethite is replaced by magnetite. Similar to the system with W/R = 10, chrysotile and magnetite are formed at a depth of 1500 m and a temperature of 116°C. The further development of mineral associations in the komatiite corresponds, in general, to that described above for depths of 3000–5600 m (237°C–440°C) in the model system with W/R = 10. The only difference in mineralogy is that quartz associates with antigorite and fayalite in the system with W/R = 1 at depths of 3550–4570 m (278°C–359°C).

The character of variations in the contents of dissolved gases and cations in hydrothermal fluid in the model system with W/R = 1 is not significantly different from the trends obtained for higher W/R. Noteworthy is only the more intense Mg removal from the fluid at a wider temperature range and higher pH values of the fluid interacting with komatiites at depths of 1500–2500 m (116°C–197°C). The compositional characteristics of hydrothermal fluid in the root part of the downwelling limb are almost identical for both W/R ratios.

Under both the scenarios considered here, the hydrothermal fluid that passed through the downwelling limb of the hydrothermal cell shows elevated (compared with initial seawater) Na, Ca, and Si, but low Mg and Al contents in the regions of its discharge on the seafloor.

INTERPRETATION OF THE RESULTS OF MODELING AND CONCLUSIONS

The obtained model data on the chemical evolution of a komatiitic material affected by a fluid of marine origin allow us to estimate the physicochemical parameters of the hydrothermal process controlling the formation of the products of the hydrothermal alteration of the earth's protocrust and reconstruct mineralogical and geochemical

Table 3. Variations in the mineral composition of komatiite and the composition of hydrothermal fluid in the downwelling limb of a model hydrothermal reactor at W/R = 10

T°C–*P*, bar (depth)	Mineral composition	Typical association	pH	SO_4 mol/kg	CO_2 mol/kg	H_2S mol/kg	H_2 mol/kg	CH_4 mol/kg	Mg mol/kg	Fe mol/kg	Ca mol/kg	Na mol/kg
35–31* (508 m)	*Qtz* + *Fe-Chl(Daf)* + *Mst* + + *Gt* + *Pyr*	*Qtz-Gt-Pyr*	5.22	1.29E-01	2.51E-01	2.40E-10	5.11E-13	8.35E-18	3.92E-01	1.81E-02	0.0030	0.0021
76–294 (1016 m)	*Qtz* + *Ang* + *Mg-Chl(Clr)* + + *Fe-Chl(Daf)* + *Mst* + *Hem* + + *Mg-Sap* + *Pyr*	*Qtz-Mgst-Hem-Pyr*	5.00	9.60E-02	8.49E-02	1.51E-08	2.19E-11	2.13E-16	3.44E-01	4.26E-04	0.0118	0.0022
116–456 (1523 m)	*Chr* + *Mg-Chl(Clr)* + + *Fe-Chl(Daf)* + *Ca* + *Mt* + *Pyr*	*Chr-Mt*	9.10	1.29E-03	5.37E-07	5.52E-04	1.64E-07	4.22E-13	9.41E-09	5.45E-08	0.1445	0.0025
156–619 (2031 m)	*Br* + *Chr* + *Mg-Chl* + + *Fe-Act* + *Mt* + *Tr*	*Chr-Mt***	9.74	1.35E-15	5.42E-12	3.49E-03	2.26E-03	1.21E-05	7.62E-10	2.25E-07	0.2227	0.0029
197–781 (2539 m)	*Br* + *Chr* + *Mg-Chl* + + *Fe-Act* + *Mt* + *Prt* + *Tr*	*Chr-Mt-Prt*	7.04	2.72E-25	2.14E-20	6.82E-05	2.19E-01	1.21E-05	3.31E-05	2.12E-06	0.1313	0.0042
237–944 (3047 m)	*Br* + *Chr* + *Fe-Chl* + *Fe-Serp* + + *Fe-Act* + *Mt* + *Prt* + *Tr*	*Chr-Mt-Prt*	5.96	2.13E-26	5.09E-20	4.79E-05	4.27E-01	1.23E-05	4.06E-04	1.96E-05	0.1282	0.0092
278–1106 (3555 m)	*Qtz* + *Ant* + *Br* + *Mg-Chl(Clr)* + + *Fe-Chl(Daf)* + *Fe-Act* + + *Mt* + *Tr*	*Ant-Mt*	5.58	3.91E-29	1.23E-21	4.88E-05	4.46E-01	1.25E-05	8.33E-03	5.56E-05	0.1174	0.0199
318–1269 (4063 m)	*Qtz* + *Ant* + *Br* + *Mg-Chl(Clr)* + + *Fe-Chl(Daf)* + *Fe-Act* + *Fa* + + *Mt* + *Tr*	*Ant-Mt-Fa*	4.67	2.29E-32	5.93E-23	4.99E-05	4.12E-01	1.29E-05	9.12E-03	4.17E-04	0.1101	0.0350
359–1431 (4570 m)	*Ant* + *Br* + *Mg-Chl* + *Fe-Act* + + *Fa* + *Mt* + *Ta* + *Tr*	*Ant-Mt-Fa*	5.50	6.44E-33	2.25E-24	5.00E-05	3.99E-01	1.30E-05	1.82E-03	1.30E-04	0.1133	0.0480
399–1594 (5078 m)	*Ant* + *Br* + *Mg-Chl* + *Fe-Act* + + *Fa* + *Mt* + *Ta* + *Tr*	*Ant-Mt-Fa-Ta*	4.82	5.29E-14	9.36E-08	1.45E-01	5.35E-02	1.30E-05	1.59E-03	6.05E-05	0.1063	0.0639
439–1756 (5586 m)	*Br* + *Mg-Chl* + *Fe-Act* + *Fa* + + *Mt* + *Ta* + *Tr*	*Mt-Fa-Ta*	4.42	5.49E-16	2.42E-08	2.55E-02	1.92E-01	1.31E-05	4.20E-03	1.18E-02	0.0966	0.0280

Note: Here and in Table 4, mineral abbreviations: *Act* is actinolite, *Ang* is anhydrite, *Ant* is antigorite, *Br* is brucite, *Ca* is calcite, *Chl* is chlorite (*Clr*—clinochlore and *Daf*—daphnite), *Chr* is chrysotile, *Dol* is dolomite, *Fa* is fayalite, *Gt* is goethite, *Hem* is hematite, *Mst* is magnesite, *Mt* is magnetite, *Prt* is pyrrhotite, *Pyr* is pyrite, *Qtz* is quartz, *Sap* is saponite, *Ta* is talc, and *Tr* is tremolite.

* Temperature and pressure values were calculated as average for model blocks.

** Ca-amphibole is stable starting from these level downsection (up to 439°C).

Table 4. Variations in the mineral composition of komatiite and the composition of hydrothermal fluid in the downwelling limb of a model hydrothermal reactor at W/R = 1

T°C–*P*, bar (depth)	Mineral composition	Typical association	pH	SO_4 mol/kg	CO_2 mol/kg	H_2S mol/kg	H_2 mol/kg	CH_4 mol/kg	Mg mol/kg	Fe mol/kg	Ca mol/kg	Na mol/kg
35–31 (508 m)	*Fe-Chl* + *Mg-Chl* + *Gt* + + *Mg-Sap* + *Pyr*	*Sap-Gt-Pyr*	5.99	1.09E-02	2.51E-03	4.1E-10	2.3E-12	2.38E-17	1.45E-01	8.20E-04	0.0016	0.0215
76–294 (1016 m)	*Mg-Chl(Chl)* + *Dol* + *Hem* + + *Mg-Sap* + *Pyr*	*Sap-Dol-Hem-Pyr*	5.73	6.31E-03	2.51E-03	1.3E-08	8.6E-11	1.09E-15	9.78E-02	1.80E-04	0.0413	0.0216
116–456 (1523 m)	*Ang* + *Br* + *Chr* + *Mg-Chl* + + *Ca* + *Mt* + *Pyr*	*Chr-Mt*	10.41	1.81E-03	3.11E-07	0.00778	6.3E-07	2.86E-13	5.20E-08	2.21E-06	0.2184	0.0221
156–619 (2031 m)	*Br* + *Chr* + *Mg-Chl* + + *Fe-Act* + *Mt* + *Tr*	*Chr-Mt**	10.13	6.66E-17	1.72E-13	0.01131	0.00818	1.19E-05	3.12E-08	4.68E-07	0.3043	0.0224
197–781 (2539 m)	*Br* + *Chr* + *Mg-Chl* + + *Fe-Act* + *Mt* + *Prt* + *Tr*	*Chr-Mt-Prt*	9.00	4.19E-20	2.86E-17	0.0068	0.11197	1.19E-05	5.91E-09	3.00E-05	0.1960	0.0232
237–944 (3047 m)	*Br* + *Chr* + *Fe-Chl* + + *Mg-Chl* + *Fe-Act* + *Mt* + *Tr*	*Chr-Mt*	6.31	1.33E-25	8.11E-20	5.7E-05	0.39248	1.25E-05	4.48E-04	5.91E-06	0.1237	0.0278
278–1106 (3555 m)	*Qtz* + *Ant* + *Br* + *Mg-Chl* + + *Fe-Chl* + *Fe-Act* + *Mt* + *Tr*	*Qtz-Ant-Mt*	5.35	2.23E-29	1.56E-21	5.8E-05	0.4213	1.27E-05	5.37E-03	1.28E-04	0.1134	0.0394
318–1269 (4063 m)	*Qtz* + *Ant* + *Br* + *Mg-Chl* + + *Fe-Chl* + *Fe-Act* + *Fa* + + *Mt* + *Tr*	*Qtz-Ant-Mt-Fa*	4.48	1.42E-32	5.55E-23	5.9E-05	0.41947	1.29E-05	1.21E-02	6.78E-04	0.0977	0.0556
359–1431 (4570 m)	*Qtz* + *Ant* + *Br* + *Mg-Chl* + + *Fe-Act* + *Fa* + *Mt* + *Tr*	*Qtz-Ant-Mt-Fa*	4.29	2.07E-34	2.14E-24	5.9E-05	0.40579	1.33E-05	1.79E-02	3.40E-03	0.0822	0.0723
399–1594 (5078 m)	*Ant* + *Br* + *Mg-Chl* + *Fe-Act* + + *Fa* + *Mt* + *Ta* + *Tr*	*Ant-Mt-Ta*	4.86	7.48E-21	2.93E-11	6E-05	0.40661	1.34E-05	9.51E-03	1.14E-03	0.0902	0.0862
439–1756 (5586 m)	*Br* + *Mg-Chl* + *Fe-Act* + *Fa* + + *Mt* + *Ta* + *Tr*	*Mt-Fa-Ta*	4.74	1.41E-19	1.21E-09	6E-05	0.40954	1.35E-05	1.70E-03	4.92E-03	0.0900	0.0973

* Ca-amphibole is stable starting from this level downsection (up to 439°C).

effects related to the activity of hydrothermal systems in the oldest oceanic basins.

Submarine Weathering on the Hadean Ocean Floor

The Archean banded iron formation (BIF) and the association of Archean volcanogenic massive sulfide (VMS) deposits [7] were formed in a subaqueous environment under the influence of two competitive processes: deposition of fine-grained mineral mats owing to the mixing of hydrothermal fluids and seawater and alteration of the newly formed mineral phases (e.g., goethite/hematite $\longrightarrow$ magnetite) owing to reactions with later hydrothermal emanations. The marine origin of the oldest metamorphosed Akilia BIF in West Greenland is supported by evidence for mass-independent isotope fractionation (MIF) of sulfur established in sulfides from these rocks [16]. This MIF was related to the transport of sulfur in the Archean from the atmosphere to the ocean and its subsequent burial in marine sediments.

The obtained results of the numerical modeling of the low-temperature alteration of komatiites on the Hadean ocean floor showed that, under relatively deep conditions (hundreds of meters, W/R = 10), an SiO_2-rich chemogenic envelope composed of strongly dominant amorphous silica, pyrite, goethite, and Fe-chlorite is formed already after several thousands of years (1000–10 000 yr) of komatiite–seawater interaction. The results of modeling suggest that the serpentinization of komatiites on the Hadean ocean floor, which was not manifested in the model system corresponding to deep basins, occurs in a shallow marine basin after 1 Ma of its existence. The model mineral transformations of the komatiite crust owing to its submarine weathering are in good agreement with the available data on the mineralogy of the comprehensively studied oldest BIF complexes: quartz + magnetite and iron-rich antigorite (greenalite) + talc (minnesotaite) in the BIF of the Isua greenstone belt (SW Greenland, >3.7 Ga) [17, 18] and magnetite + quartz + hematite + carbonate in the BIF of the Jharkhand–Orissa supracrustal complex (India) [19]. The verisimilitude of the volume proportions of the newly formed minerals in the altered komatiitic material obtained by modeling is supported by the data on the bulk composition of natural BIF: 98–99 wt % of SiO_2 and Fe_2O_3 in the Jharkhand–Orissa quartzites [19] and 10–50 wt % Fe_2O_3 and 40–80 wt % SiO_2 in the quartzites of the Nkonga and Pongola complexes (Kaapvaal craton) [20].

The results of our modeling can be used for the interpretation of the conditions of formation of various mineral types of BIF and associated rocks. It is evident that the most typical mineral varieties of Archean iron formations composed of quartz, hematite, and magnetite were rather rapidly (≤100000 yr) formed at the low-temperature alteration of rocks on the floor of a relatively deep (at least hundreds of meters) marine basin. This interpretation is in agreement with the results of the investigation of fluid inclusions in quartz filling voids and fractures in the oldest pillow lavas of southern Africa (Barberton), Western Australia (Pilbara), and Canada (Abitibi), which indicates that these rocks associating with iron formation underwent halmyrolysis in marine basins deeper than 200 m [21]. The minimum water depth during the formation of the Ironstone BIF (Barberton, southern Africa) was estimated as approximately 980 m from the homogenization temperature and the composition of gases in fluid inclusions [22].

According to the results of calculations, the BIF complexes associating with serpentinized komatiites were formed after prolonged (>100 000 yr) low-temperature komatiite–seawater interaction in shallow basins (no more than a few tens of meters).

The model calculations established that the pH value of the primordial hydrosphere interacting with a komatiitic material already increases significantly after 4000 model years of the existence of the marine basin. This effect is supported by the concept that the initial hydrosphere showed low pH, but it was neutralized owing to interaction with the earth's protocrust (e.g., [21, 23]). The results of modeling favor the rapid extraction of cations (Mg, Ca, and Na) from the protocrust into primary seawater. Perhaps, already 100 000 yr after the beginning of submarine weathering, the seawater of the oldest oceanic basins was similar in composition to modern seawater. Our calculations suggest that, in contrast to the waters of relatively deep marine basins, the water of shallow reservoirs is mineralized much faster and has a higher sodium concentration. This inference is supported by the analysis of the composition of fluid inclusions in the minerals of the oldest oceanic crustal complexes, which showed that the hydrosphere of the Archean deep-sea basins contained from 8 to 12 wt % NaCl, whereas the content of NaCl could be as high as 25 wt % in the shallow basins where evaporates were accumulated [21].

The modeling showed that the content of CO_2 in the primordial atmosphere decreased considerably 100 000 model years after the formation of the earliest marine basins. Simultaneously, the chemical interaction of the hydrosphere with the komatiitic crust resulted in the extensive formation of carbonates.

It is supposed that the development of BIF involved the activity of cyanobacteria, which promoted Fe^{2+} oxidation (e.g., [24]). Calculations based on experimental data on the rate of ferrous iron oxidation under the influence of cyanobacteria under lighting conditions corresponding to ocean depths of a few hundreds of meters allowed us to suggest that anaerobic phototrophic organisms could be among the main agents of BIF deposition on the floor of the ancient ocean and responsible for the absence of dissolved Fe in its surface water layer [25]. The earliest evidence for the existence of microorganisms was found in the oldest crustal materials with ages of 3.8–3.85 Ga: BIF of Isua and Akilia in southwestern Green-

land [8]. The isotopic composition of C was determined in microscopic fragments of elemental carbon from inclusions in apatite using an ion microprobe. It was found that the $\delta^{13}C$ of this material corresponds to values typical of ancient and modern microorganisms (from −50 to −20) [6]. The influence of the biogenic factor on the origin of BIF was also established for the Pongola and Nkonga complexes of the Kaapvaal craton, southern Africa. The carbonate phase of these rocks shows δC^{13} values from −9.12 to −15.70@ [20]. On the other hand, Whitehouse [18] determined the isotopic composition of iron in magnetite from the oldest BIF of the Isua complex by secondary ion mass spectrometry (SIMS) and advocated the abiogenic origin of these rocks. It should be noted that the iron isotopic composition of the Isua BIF reported in [18] should be interpreted taking into account that the modern structure of the quartzites was formed by the high-grade regional metamorphism of the protolith of these rocks. This protolith was metamorphosed under redox conditions different from those during its formation in an oceanic environment, which had to affect the behavior of the iron isotope system in these rocks.

Hydrothermal Process within the Crustal Section of the Hadean Ocean

The results of the modeling of hydrothermal circulation within the Hadean protocrust of the ancient ocean demonstrated that the W/R ratio significantly affects the geochemical and mineralogical features of the model system only in the upper part of the crustal section, up to a depth of 1500 m and a temperature of 116°C. This conclusion is clearly illustrated by the sequence of mineral transformations in the komatiite material for the selected W/R values (1 and 10) (Tables 3, 4). The obtained data allow us to distinguish the following characteristic mineral facies of hydrothermally altered komatiites constituting the protocrust of the Hadean ocean for the temperature range 35°–439°C and W/R of 10 and 1 (mineral symbols are given in Table 3):

$$\text{(W/R = 10) I. } Qtz + Gt + Pyr \longrightarrow \text{II. } Qtz + Mgst + Hem + Pyr \longrightarrow \text{III. } Chr + Mt \longrightarrow \text{IV. } Ant + Mt + Fa \longrightarrow \text{V. } Mt + Fa + Ta\ ;$$

$$\text{(W/R = 1) I. } Sap + Gt + Pyr \longrightarrow \text{II. } Sap + Dol + Hem + Pyr \longrightarrow \text{III. } Chr + Mt \longrightarrow \text{IV. } Ant + Mt + Fa + Qtz \longrightarrow \text{V. } Mt + Fa + Ta.$$

It should be noted that calcic amphibole (actinolite–tremolite) is formed in hydrothermally altered komatiite in both model systems starting from a temperature of 156°C. This mineral is traced downsection to a depth of 5600 m (439°C). In the low-W/R system, brucite crystallizes within a wider temperature range compared with the system with W/R = 10. Within mineral assemblage (III), pyrite is replaced by pyrrhotite in the two model systems at a temperature of 197°C.

Our modeling of hydrothermal alteration in the peridotites of modern MOR showed that three redox regimes can be distinguished in an oceanic crustal section composed of ultrabasic rocks at depths from the ocean floor to approximately 6 km: (1) strongly oxidized (near the surface) with the characteristic association aragonite + goethite; (2) moderately oxidized (fluid-dominated), serpentine + chlorite + hematite + pyrite (*Mt–Hem* buffer); and (3) reduced (rock-dominated), serpentine + olivine + magnetite + pyrrhotite (QFM buffer) [12]. The results of calculations described above indicate that the fluid regime that developed during the hydrothermal alteration of the ancient komatiite material was similar to that observed in modern hydrothermal systems in the peridotites of the oceanic crust. The mineral facies distinguished above for hydrothermally altered komatiites can be correlated with the types of redox regime in the following manner: (1) strongly oxidized (near-surface)—I, (2) moderately oxidized (fluid-dominated)—II, and (3) reduced (rock-dominated)—III–V.

The compositional evolution of hydrothermal fluid during its percolation through the komatiitic section reflects changes of mineral facies in the country rocks: the extensive enrichment of the fluid in H_2S, CH_4, and H_2 and the loss of SO_4 begin from the depth level corresponding to the replacement of hematite by magnetite and the appearance of chrysotile in the rock, i.e., a transition from facies II to facies III. The hydrothermal fluid loses CO_2 within the whole range of depths in the upper part of the section, where magnesite and calcite are formed (facies II). The almost complete loss of sulfate from the fluid is observed at a temperature of approximately 240°C, i.e., at the level where, according to the calculations, the precipitation of sulfides (represented here by pyrrhotite) is terminated in the section. A considerable Mg removal from the fluid and an increase in its pH are confined to the section level corresponding to the beginning of the extensive serpentinization of komatiite (facies III).

The mineral associations of hydrothermally altered komatiites obtained in the numerical model are consistent with the phase compositions of metamorphosed komatiites from the oldest greenstone belts, for instance, Agnew–Wiluna in the Yilgarn block, Western Australia [26]. Sulfides are formed in the model system within the whole range of *P–T* conditions considered, irrespective of the W/R value; therefore, it is instructive to compare the results of modeling with data on the composition of the earliest VMS-type mineralization. It is commonly accepted that VMS-type deposits were formed owing to the activity of hydrothermal systems located within volcanic sequences beneath the ocean floor (e.g., [27]). When hydrothermal fluid discharges onto the ocean floor, it is mixed with seawater and cools, which results in the deposition of sulfides forming ore bodies. The best studied Archean VMS are the sulfide–base metal deposits of the Pilbara and Yilgarn cratons (Western Australia). The typical association of ore occurrences related to these depos-

its is pyrite + quartz + chalcopyrite [27]. Vein mineralization is widespread in the VMS of the Pilbara and Yilgarn cratons; the veins are made up of quartz, pyrite, chalcopyrite, and minor sphalerite and carbonate [28]. The vein mineral assemblage includes also magnetite and talc. The Early Archean (3.26 Ga) massive sulfide deposits in the eastern part of the Pilbara craton are located within the Strelly greenstone belt and preserved clear textural characteristics of sulfide ores identical to those observed in the modern ore structures of black smokers in MOR [28].

The results of the modeling of hydrothermal systems in the ancient ocean suggest that the vein mineralization observed in the Archean VMS deposits of Western Australia was related to the hydrothermal alteration of ancient volcanic rocks under oxidized–moderately oxidized fluid conditions within the fields of facies I and II (facies V in the presence of talc) at $W/R \geq 10$.

There is evidence for the participation of living organisms in the earliest hydrothermal systems on earth. Rasmussen [29] reported the first data on fibrous pyrite aggregates from the Sulfur Springs VMS deposit (Pilbara craton) with an age of 3.24 Ga, which are probably fossil remnants of the earliest filamentous organisms. The sites of their probable residence indicate that these microorganisms could be represented by thermophile and chemotropic prokaryotes.

CONCLUSIONS

Based on our modeling of interaction between the komatiitic protocrust of the earth's oldest oceans and the hydrosphere, the following tentative conclusions were drawn on the probable geochemical effects accompanying the early evolution of the atmosphere, hydrosphere, and lithosphere.

(1) The protolith of the oldest sedimentary sequences on earth (BIF) could be formed in relatively deep basins already after a few thousand years of low-temperature interaction between the komatiitic crust and aqueous solution.

(2) The serpentinization of komatiites was not characteristic of the crust of deep ancient basins but was possible in shallow reservoirs, where it developed 1 Ma after their formation.

(3) During interaction with the komatiitic crust, the pH value of the early hydrosphere already increased significantly after 4000 yr of its existence. The hydrosphere rapidly extracted Mg, Ca, and Na from the protocrust, and the mineralization of seawater probably approached the modern value already 100 000 yr after the beginning of submarine weathering.

(4) The balance of CO_2 in the atmosphere–hydrosphere–crust system strongly depended on the character of mineral formation during the alteration of the crustal material owing to its interaction with seawater. A sharp depletion of the earth's early atmosphere in CO_2 began probably 100 000 yr after the formation of the hydrosphere and reflected the stage of extensive formation of the earliest carbonates in the hydrothermally altered crust.

(5) Hydrothermal fluid passing through the downwelling limb of a hydrothermal cell is enriched relative to the initial hydrosphere in Na, Ca, and Si, whereas Mg is consumed for serpentinization during the transport of the fluid through the komatiitic section.

(6) Vein mineralization observed in Archean VMS (volcanic massive sulfide) deposits was related to the hydrothermal alteration of ancient volcanic rocks under oxidized–moderately oxidized fluid conditions at $W/R \geq 10$.

ACKNOWLEDGMENTS

We thank M.V. Mironenko for providing programs, consultations, and insightful discussion.

This study was financially supported by program no. 15 of the Presidium of the Russian Academy of Sciences, subprogram 1, theme "Reconstruction of the Formation Conditions of the Protocrust of the Early Earth and Its Role in the Evolution of the Composition of the Primary Atmosphere and Hydrosphere."

REFERENCES

1. M. Ozima and F. A. Podosek, "Formation Age of the Earth from $^{129}I/^{127}I$ and $^{244}Pu/^{238}U$ Systematics and the Missing Xe," J. Geophys. Res. **104** (B11), 25493–25499 (1999).
2. J. W. Valley, W. H. Peck, E. M. King, and S. A. Wilde, "A Cool Early Earth," Geology **30**, 351–354 (2002).
3. E. M. Galimov, "Redox Evolution of the Earth Caused by a Multi-Stage Formation of Its Core," Earth. Planet. Sci. Lett **233**, 263–276 (2005).
4. G. Caro, B. Bourdon, J.-L. Birck, and S. Moorbath, "High-Precision $^{142}Nd/^{144}Nd$ Measurements in Terrestrial Rocks: Constraints on the Early Differentiation of the Earth's Mantle," Geochim. Cosmochim. Acta **70**, 164—191 (2006).
5. S. B. Shirey, U. Wiechert, R. W. Carlson, et al., "Re–Os and Oxygen Isotopic Systematics of Diamondiferous and Non-Diamondiferous Eclogites from the Roberts Victor Kimberlite, South Africa," in *Ninth Annual V.M. Goldschmidt Conference, Houston, Texas, 1999* Lunar Planet. Inst. Contrib. **971**, 273–274 (1999).
6. H. Ohmoto, "Banded Iron Formations as Guides for the History of the Lithosphere, Atmosphere, and Hydrosphere," GSA Denver Annual Meeting, Abstract Volume, No. 125, 9 (2002).
7. S. J. Mojzsis, G. Arrhenius, K. D. McKeegan, et al., "Evidence for Life on Earth before 3800 Million Years Ago," Nature **384**, 55–59 (1996).
8. J. M. Franklin and M. Hannington, "Volcanogenic Massive Sulfides through Time," GSA Denver Annual Meeting, Abstract Volume, No. 125, 7 (2002).
9. M. Nedachi and H. Ohmoto, "2.76 Ga Submarine Hydrothermal System Associated with Life in the Mt. Roe Basalt, Pilbara, Australia," GSA Denver Annual Meeting, Abstract Volume, No. 226, 8 (2002).

10. M. V. Mironenko, T. Yu. Melikhova, M. Yu. Zolotov, and N. N. Akinfiev, "GEOCHEQ_M—the Complex for Thermodynamic and Kinetic Modeling of Geochemical Processes. Version of 2008," Vestn. Otd. Nauk Zemle RAN **1** (26), (2008). URL: http://www.scgis.ru/russian/cp1251/h_dgggms/1-2008/informbul-1_2008/Mineral-22.pdf.
11. M. Y. Zolotov and M. V. Mironenko, "Timing of Acid Weathering on Mars: A Kinetic-Thermodynamic Assessment," J. Geophys. Res. **112**, E07006 (2007).
12. S. A. Silantyev, M. V. Mironenko, and A. A. Novoselov, "Hydrothermal Systems in Peridotites of Slow-Spreading Mid-Oceanic Ridges. Modeling Phase Transitions and Material Balance: Downwelling Limb of a Hydrothermal Circulation Cell," Petrologiya **17** (2), 154–174 (2009) [Petrology **17**, 138–157 (2009)].
13. T. M. Gerlach, "Interpretation of Volcanic Gas Data from Tholeiitic and Alkaline Mafic Lavas," Bull. Volcanol. **45–3**, 235–244 (1982).
14. A. S. Monin, *History of the Earth* (Nauka, Leningrad, 1977) [in Russian].
15. N. T. Arndt and R. W. Nesbitt, "Geochemistry of Munro Township Basalts," In *Komatiites*, Ed. by N. T. Arndt and E. G. Nisbet (Allen and Unwin, London, 1982), pp. 309–329.
16. S. J. Mojzsis and T. M. Harrison, "Origin and Significance of Archean Quartzose Rocks at Akilia, Greenland," Science **298**, 917 (2002).
17. R. F. Dymek and C. Klein, "Chemistry, Petrology and Origin of Banded Iron-Formation Lithologies from the 3800 Ma Isua Supracrustal Belt, West Greenland," Precambrian Res. **39**, 247–302 (1988).
18. M. Whitehouse, "Micro-Scale Heterogeneity and Redistribution of Iron Isotopes in Earth's Oldest Banded Iron Formation Revealed by Secondary Ion Mass Spectrometry," Eur. Sci. Found. Univ. Leeds (2007). http/www.see.leeds. ac.uk/research/igc/arcenv/new.htm
19. H. N. Bhattacharya, I. Chakraborty, and K. K. Ghosh, "Geochemistry of Some Banded Iron-Formations of the Archean Supracrustals, Jharkhand–Orissa Region. India," J. Earth Syst. Sci. **116** (3), 245–259 (2007).
20. B. Smith, "Witwatersrand and Pongola Supergroups of South Africa. Archean Environment: the Habitat of Early Life," Eur. Sci. Found. Univ. Leeds (2007). http/www.see.leeds. ac.uk/research/igc/arcenv/new.htm.
21. D. A. Banks, "The Composition and Controls of the Oceans in the Archean and Paleoproterozoic," Eur. Sci. Found. Univ. Leeds (2007). http/www.see.leeds.ac.uk/research/igc/arcenv/new.htm.
22. C. F. J. De Ronde, C. J. Bray, E. T. C. Spooner, et al., "Direct Measurements of Hydrothermal Fluids from Ancient Seafloor Vents: Implications for the Composition of Archean Seawater," GSA Denver Annual Meeting, Abstract Volume, No. 226, 6 (2002).
23. H. D. Holland, *The Chemical Evolution of the Atmosphere and Oceans* (Princeton University Press, Princeton, 1984).
24. S. Heising and B. Schink, "Phototrophic Oxidation of Ferrous Iron by a Rhodomicrobium Vannielii Strain," Microbiology **144**, 2263–2269 (1998).
25. A. Kappler, C. Pasquero, and K. O. Konhauser, "Deposition of Banded Iron Formations by Anoxygenic Phototrophic Fe(II)-Oxidizing Bacteria," Geology **33** (11), 865–868 (2005).
26. M. J. Gole, S. J. Barnes, and R. E. T. Hill, "The Role of Fluids in the Metamorphism of Komatiites, Agnew Nickel Deposit, Western Australia," Contrib. Mineral. Petrol. **96**, 151–162 (1987).
27. M. E. Barely, "Archaean Volcanic-Hosted Massive Sulphides," AGSO J. Austral. Geol. Geophys. **17** (4), 69–73 (1998).
28. S. Vearncombe, M. E. Barley, D. I. Groves, N. J. Mc Naughton, E. J. Mikucki, and J. R. Vearncombe, "3.26 Ga Black Smoker-Type Mineralization in the Strelly Belt, Pilbara Craton," West. Austral. J. Geol. Soc. **152** (4), 587–590 (1995).
29. B. Rasmussen, "Filamentous Microfossils in a 3.235-Million-Year-Old Volcanogenic Massive Sulphide Deposit," Nature **405**, 676–679 (2000).